

Improving Trajectory Tracking for Systems with Unobservable Modes Using Command Generation

Erika Biediger, Jason Lawrence, and William Singhose

Abstract—Trajectory tracking with flexible systems is extremely difficult. This difficulty is increased when there are unobservable modes. Optimal PID control can be used for standard trajectory tracking, whereas sliding mode control can be used in systems with parametric uncertainties. Command shaping has been proven to be beneficial in eliminating unwanted vibration. This paper shows that command generation can be utilized to eliminate unwanted vibration from a system with an unobservable mode. Both optimal PID and sliding mode control can be used in conjunction with command generation for enhanced system performance.

I. INTRODUCTION

As machines are pushed to their operational limit, they often start to vibrate. If these detrimental vibrations are unobservable to the feedback control system, then they can be extremely challenging to suppress. Examples of such machines include x-y stages, coordinate measuring machines, and gantry machines. Many times during the operation of these machines, there is an additional flexible body that is attached to the system, such as a tool attached to the end of a robotic arm. The base system's position and velocity are accurately known; however, there is no real-time state information available for the attached additional mode.

For the purpose of this paper, the following types of modes are considered as unobservable:

- 1) Modes that are truly unobservable
- 2) Theoretically observable modes that are not observable in practice due to:
 - Sensor noise
 - Sensor resolution

Two prominent feedback methods are examined in this study: PID and sliding mode control (SMC). However both of these control methods have limited utility for controlling systems with unobservable modes.

A. PID Control

PID control is the most widely used form of feedback control. By optimizing the PID gains one can often design a versatile, high performance controller with good trajectory tracking, fast response time, low overshoot, and minimal

E. Biediger is a graduate student in Mechanical Engineering, Georgia Institute of Technology, Atlanta Georgia gte377k@mail.gatech.edu

J. Lawrence is a graduate student in Mechanical Engineering, Georgia Institute of Technology, Atlanta Georgia gte867w@mail.gatech.edu

W. Singhose is a professor in Mechanical Engineering, Georgia Institute of Technology, Atlanta Georgia bill.singhose@me.gatech.edu

steady state error. However, the success of PID control requires the sensor to feedback information about the system. If the system contains any unobservable modes, the PID control will not be able to compensate for errors in such modes.

B. Sliding Mode Control

The main purpose of sliding mode control (SMC) is to reject disturbances and to remain insensitive to parameter uncertainties [1]. Sliding mode control can produce perfect trajectory tracking even in the presence of parameter uncertainties [2]. In order to keep the system response along the desired trajectory, the actuator is forced to rapidly switch between full positive and full negative effort. The constant switching of the actuator effort often results in chatter, which may excite unmodeled or unobservable modes and result in large endpoint tracking error. It is possible to eliminate the chattering by using piece-wise continuous approximation of the discontinuous control law and a boundary layer [1–6]. Often times a linear approximation of the jump discontinuity is used [1–3, 5]. The width of the boundary layer determines how much the actuator will chatter. Many times, the width of the boundary layer is found by trial and error; however, methods for tuning the width of the boundary layer in addition to other SMC parameters have been developed [3].

C. New Control Scheme

Given the difficulty caused by unobservable modes, it is natural to search for a complimentary method that can enhance different feedback control systems. One promising technique is a command shaping scheme that reduces residual vibration. Command shaping does not use any feedback information, making it an ideal choice for systems with unobservable modes. It only uses estimates of the system's natural frequencies and damping ratios. This technique will be further discussed in Section II.

Given the aforementioned benefits of command shaping, the authors propose that the control structure shown in Fig. 1 be used for systems with unobservable modes. Notice that this structure uses both an command shaper and a feedback controller. For the purposes of this study, it is assumed that the feedback controller block is either a PID or SMC controller. However, the ideas presented here could easily be extended to other feedback controllers.

If the controller gains are chosen correctly then the control structure shown in Fig. 1 will utilize the strengths of both the feedback and command generator blocks. The

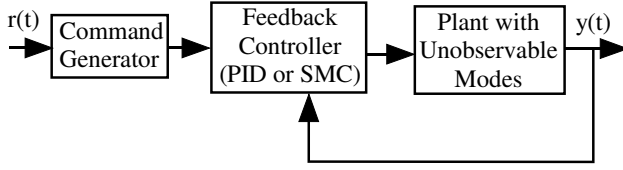


Fig. 1. Using Command Generation on a Step Input

command generator block will eliminate vibration from the unobservable modes. The feedback controller will provide accurate positioning and disturbance rejection in the case of the PID controller; and compensate for modeling uncertainties for the case of the SMC controller. However the question arises; how should the feedback and command generator parameters be chosen to implement such a scheme?

This study presents a simple, yet effective way to choose the parameters for the system shown in Fig. 1:

- 1) Design the feedback (PID or SMC) controller for the observable modes.
- 2) Design the command generator for the unobservable modes, independent of the feedback design.

This two-part design procedure implies that the feedback and command generator blocks can be designed independently of one another. This paper demonstrates that this simple design procedure is extremely effective.

The remainder of the paper is divided into the following sections: Section II reviews the basic concepts of Command Generation. Section III discusses a benchmark system. The proposed control scheme will then be implemented using PID control in section IV and SMC control and section V. In both cases the benefits of using the command generator block are highlighted in the discussion. Finally section VI presents the conclusions.

II. COMMAND SHAPING REVIEW

Command generation was first developed in the 1950's [7]. Unfortunately, the early methods were extremely susceptible to modelling errors and the lack of digital computers hampered the application of these techniques. However, there was a resurgence of interest in command shaping [8] when digital computers became widespread and a robust method was developed [9]. Command shaping has been implemented on a variety of systems including robotic manipulators [10, 11], cranes [12, 13], milling machines [14], and coordinate measuring machines [15–17].

Command shaping is implemented by convolving a sequence of impulses, called the command shaper, with any desired reference command [9]. The convolved signal is then used as the new reference command for the system. Fig. 2 demonstrates the process with a step input and a command shaper containing three positive impulses. The resulting shaped input is a three-step staircase command. It is important to note that the shaping process increases the rise time of the command by the duration of the shaper.

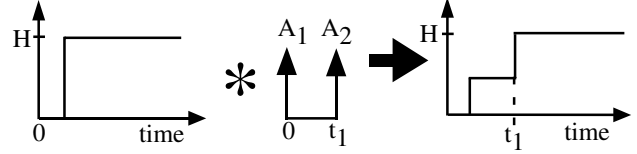


Fig. 2. Command Shaping a Step Input

The amplitudes and time locations of an command shaper's impulses are determined by satisfying constraint equations. The amplitudes and time locations for the Zero Vibration (ZV) shaper are known in closed form and are calculated from [9]:

$$\begin{bmatrix} A \\ t \end{bmatrix} = \begin{bmatrix} \frac{1}{1+K} & \frac{K}{\frac{1+K}{\pi}} \\ 0 & \frac{K^2}{\omega\sqrt{1-\zeta^2}} \end{bmatrix} \quad (1)$$

The Zero Vibration and Derivative (ZVD) shaper is more robust to changes in the system's natural frequency and damping ratio than the ZV shaper [9]. The amplitudes and time locations for this shaper are found by solving the same constraint equations used for the ZV shaper and an additional constraint which forces the derivative of the vibration to be zero at the modeled frequency. The amplitudes and time locations can be calculated from:

$$\begin{bmatrix} A \\ t \end{bmatrix} = \begin{bmatrix} \frac{1}{1+2K+K^2} & \frac{2K}{\frac{1+2K+K^2}{\pi}} & \frac{K^2}{\frac{1+2K+K^2}{2\pi}} \\ 0 & \frac{K^2}{\omega\sqrt{1-\zeta^2}} & \frac{K^2}{\omega\sqrt{1-\zeta^2}} \end{bmatrix} \quad (2)$$

where

$$K = e^{-\frac{\zeta\pi}{\sqrt{1-\zeta^2}}} \quad (3)$$

Other constraints such as additional robustness, limits on the magnitudes of the impulses, and/or time optimality requirements can also be used to calculate the amplitudes and time locations for a shaper [18].

III. MODEL DESCRIPTION

Fig. 3 represents the benchmark system used to test the control scheme in Fig. 1. The equations of motion for the system are:

$$\ddot{x}_1 = \frac{1}{m_1} [u - k_1 x_1 - b_1 \dot{x}_1 + k_2 (x_2 - x_1) + b_2 (\dot{x}_2 - \dot{x}_1)] \quad (4)$$

$$\ddot{x}_2 = \frac{1}{m_2} [-k_2 (x_2 - x_1) - b_2 (\dot{x}_2 - \dot{x}_1)] \quad (5)$$

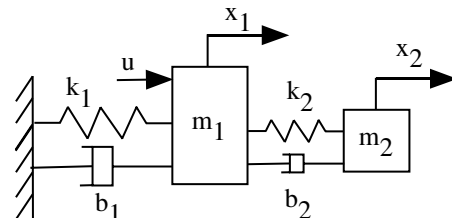


Fig. 3. Full-Order System Model

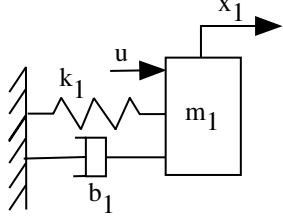


Fig. 4. Reduced-Order System Model

The benchmark system consists of two parts: the observable mode, and the unobservable mode. The observable mode can be isolated from the full system and redrawn as the reduced-order system shown in Fig. 4. This reduced-order system is used for designing the feedback controllers. The equation of motion for the reduced-order system is:

$$\ddot{x}_1 = \frac{u}{m_1} - \frac{k_1}{m_1}x_1 - \frac{b_1}{m_1}\dot{x}_1 \quad (6)$$

The unobservable mode is represented as a second mass-spring-damper system whose mass parameters are significantly smaller than the primary mass, m_1 . This mode can be used to represent a tool or device attached to the end effector of a machine. As discussed in the introduction, the unobservable mode parameters will be used to design the command generator and have no effect on the feedback controller design.

Both PID and SMC algorithms will be tested as possible feedback control elements for the full-order system. For the PID case we assume that all system parameters are known, and are given in Table I. The unobservable mode has a damping ratio of 0.05 and a natural frequency of approximately 1.6 Hz. Note that the parameters were chosen to yield a lightly damped, second mode with very little coupling to the primary mode. Also the maximum actuator effort for the system, u_{max} , is given. For the SMC case we assumed that the parameters of the observable mode are only known within a range, given in Table II. The goal is for both masses, m_1 and m_2 , to follow the trapezoidal position trajectory shown in Fig. 5. As seen in the figure, the trajectory can be characterized as a ramp-wait-return maneuver. This type of trajectory could be used for manufacturing processes such as pick-and-place motions. Basically, the machine would be required to follow a constant velocity path until it stops at the desired location

TABLE I
FULL SYSTEM PARAMETERS

m_1	m_2	k_1	k_2	b_1	b_2	u_{max}
5 kg	0.1 kg	5.5	10	0.9	0.1	75 N

TABLE II
PARAMETER RANGES FOR SMC CASE.

m_{low}	m_{high}	k_{low}	k_{high}	b_{low}	b_{high}
2 kg	8 kg	1	10	0.5	1.3

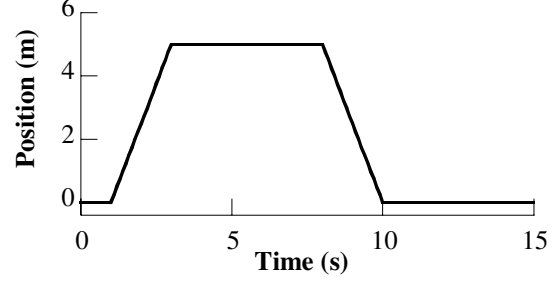


Fig. 5. Ramp-Wait-Return Trajectory

for a specified amount of time. It is during this wait time that a process would be completed. Once the wait portion of the command is over, the system follows the desired path back to the starting position. Trajectory tracking refers to the error over the entire cycle. During the wait portion of the maneuver, the system should maintain the desired position with near zero velocity and acceleration while it is completing some process.

IV. COMMAND GENERATION WITH AN OPTIMAL PID CONTROLLER

A. Optimizing the PID Gains for the Reduced-Order Model

As explained previously, a two part approach will be used to design the controller. In the first part of the design process an optimal PID controller is designed for the observable mode. For this portion of the design process we only use the reduced-order system given in Fig. 4. To find the optimal set of PID parameters the problem was formulated as follows:

$$\begin{aligned} \min [e] &= \int_0^{t_f} (x_1(t) - x_d(t))^2 dt \\ \text{such that: } \max |F(t)|_0^{t_f} &< F_{limit} \end{aligned} \quad (7)$$

where e is the squared error, x_1 is the position of m_1 , x_d is the desired trapezoidal position trajectory shown in Fig. 5, t_f is the end time of the trajectory, and F is the actuator force. Notice that included in (7) is an actuator saturation limit, F_{limit} , which was set to 75 N. This physical system constraint keeps the optimal PID gains bounded.

The minimization problem (7) was solved using MATLAB's "fmincon" function. The minimization program also used a linear simulation routine to generate the $x_1(t)$ and $F(t)$ from the equations of motion in (6) for each trial set of gains. The MATLAB minimization routine successfully converged and the optimal PID gains were found to be: P=238, D=28, I=186.

B. System Response Using Optimized PID Gains and Command Generator

The second part of the control design process is to use command generation to eliminate vibration in the second, unobservable mode. The natural frequency and damping ratio for the unobservable mode were 1.6 Hz and 0.05 respectively. These values were substituted into equation

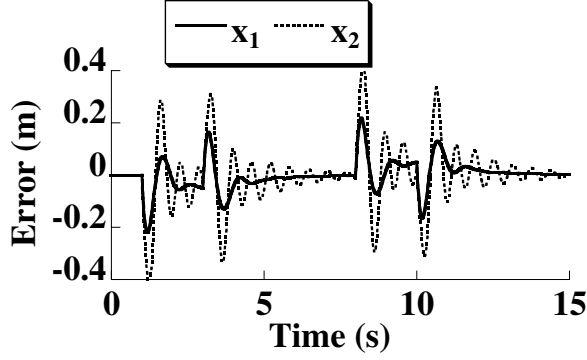


Fig. 6. PID Control System Tracking Error (No Shaping)

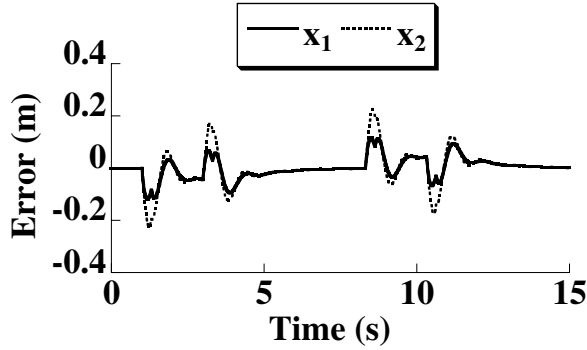


Fig. 7. PID and Command Shaping Control System Tracking Error

1 to derive a ZV shaper for the system:

$$\begin{aligned} t_1 &= 0 & A_1 &= 0.5392 \\ t_2 &= 0.3146 & A_2 &= 0.4608 \end{aligned} \quad (8)$$

As seen from (8), the ZV shaper is composed of two impulses separated by approximately 0.31 seconds.

Fig. 6 shows the error of the m_1 and m_2 responses without using any command generator. The tracking error is measured as deviation from the desired trajectory given in Fig. 5. Notice that the PID control achieves good trajectory tracking for mass m_1 . This is because mass m_1 is the observable mode. However mass m_2 has significant tracking error because it is unobservable.

Fig. 7 shows the tracking error of the m_1 and m_2 responses with the ZV command generator. Notice that the errors in both masses are small over the course of the trajectory. Comparing Figs. 7 and 6 we see that the command generator plays a significant role in reducing the error of the unobservable mode.

C. Discussion

There are ways that this controller design process could be refined to achieve even better results for some cases:

- 1) The optimal PID gains could be found for the shaped, rather than the unshaped trajectory.
- 2) A multimode command generator could be designed to also eliminate the controller dynamics. Such a command generator would not only improve the response of m_2 , but also m_1 [19].

V. COMMAND GENERATION WITH A SLIDING MODE CONTROLLER

First order systems are fairly easy to control; therefore, the basis of SMC is to replace n^{th} -order systems with an equivalent first-order system. The sliding manifold is defined as the surface of the state-space along which the sliding mode occurs, and it has been proven that the system will move toward or remain on the manifold [1]. If the system starts at any arbitrary point away from the sliding manifold, it will always move toward it after going through a transient period.

Normally, the SMC is based on the best estimation of the system model. Following [3], the sliding manifold for the reduced-order model is given by:

$$s = \dot{x}_1 + \lambda \tilde{x}_1 \quad (9)$$

where

$$\tilde{x}_1 = x_1 - x_d \quad (10)$$

x_1 = states of the system, x_d = the desired states, λ = positive constant, and n = the number of states. The equivalent control law is composed of a continuous control law approximation, \bar{u} , and a discontinuous term, $K \text{sgn} |s|$:

$$u = \bar{u} - K \text{sgn} |s| \quad (11)$$

From (11), K represents the weight of the discontinuous control effort, and is defined by [2]:

$$K = F + \eta \quad (12)$$

where F is the estimation error of the system.

The values for the mass, spring, and damper each lie within a known bounded region given by:

$$\begin{aligned} m_1 &\in [m_{low}, m_{high}] \\ k_1 &\in [k_{low}, k_{high}] \\ b_1 &\in [b_{low}, b_{high}] \end{aligned} \quad (13)$$

where \bar{m}_1 , \bar{k}_1 , and \bar{b}_1 are the average values used to construct the nominal control, \bar{u} , defined by:

$$\bar{u} = \bar{k}_1 x_1 + \bar{b}_1 \dot{x}_1 + \bar{m}_1 \ddot{x}_d - \bar{m}_1 \lambda \dot{\tilde{x}}_1 \quad (14)$$

Here F is defined using a constant uncertainty for each of the parameters, and is given by:

$$\begin{aligned} F \geq & |k_1 - \bar{k}_1| \cdot |x_1| + |b_1 - \bar{b}_1| \cdot |\dot{x}_1| + |m_1 - \bar{m}_1| \cdot |\ddot{x}_d| \\ & + |m_1 - \bar{m}_1| \cdot \lambda \cdot |\dot{\tilde{x}}_1| \end{aligned} \quad (15)$$

A. System Response Using SMC Controller and Command Generator

The controller design process described in the introduction I-C was applied to the system using a SMC feedback controller. The first part of this design process is choosing the SMC gains for the reduced-order system. As seen from (9) through (15), there are several parameters that affect the performance of the controller. All of the barred values were derived as the average value of the parameter ranges shown

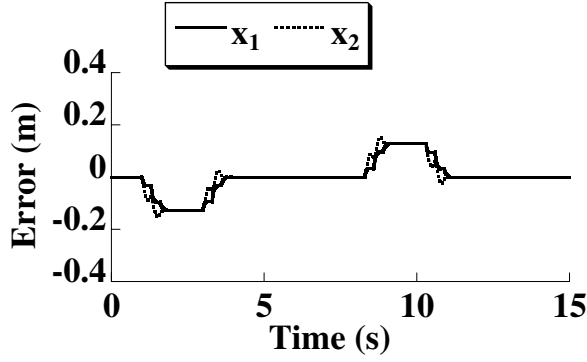


Fig. 8. SMC and ZVD Control System Tracking Error

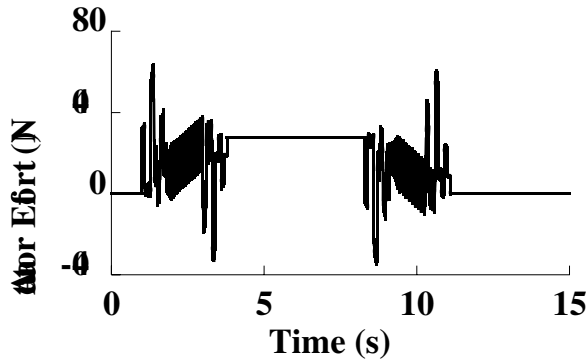


Fig. 9. SMC and ZVD Control System Actuator Effort

in Table II. The value of λ to a large extent determines how well the system tracks the desired trajectory. The larger the value of λ , the smaller the trajectory tracking error for x_1 . For the reduced-order system $\lambda=1000$ provided good tracking error without exceeding the actuator constraints. In addition η was chosen to be 0.001.

The second part of the controller design process is choosing the command generator parameters for the unobservable mode. The natural frequency and damping ratio of the unobservable mode were 1.6 Hz and 0.05 respectively. These were substituted into equation 16 to derive a ZVD shaper for the system:

$$\begin{aligned} t_1 &= 0 & A_1 &= 0.2908 \\ t_2 &= 0.3146 & A_2 &= 0.4969 \\ t_3 &= 0.6291 & A_3 &= 0.2123 \end{aligned} \quad (16)$$

Fig. 8 shows the tracking error in both masses using the SMC controller and the ZVD shaper discussed above. Note that the system exhibits good tracking in both x_1 and x_2 . Furthermore, the tracking error is far superior to the PID case previously shown in Fig. 7. The only noticeable tracking errors occur at the corners of the desired trajectory shown in Fig. 5. At these corners there are large accelerations due to discontinuous jumps in the desired velocity.

Fig. 9 shows the actuator effort for the response shown in Fig. 8. Notice that at each of the trajectory corner points,

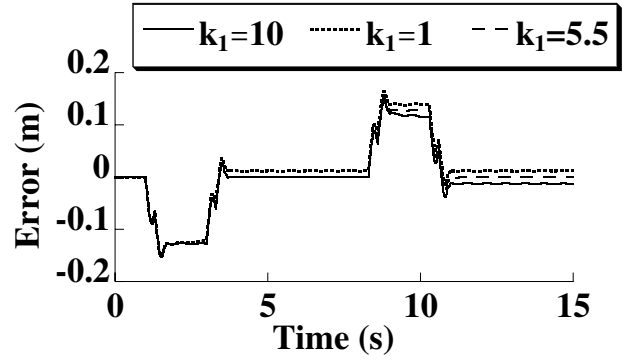


Fig. 10. SMC and ZVD Control System Tracking Error (Various k_1)

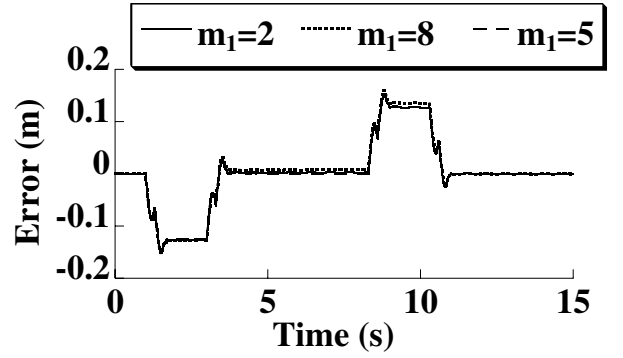


Fig. 11. SMC and ZVD Control System Tracking Error (Various m_1)

the actuator effort spikes and then displays the jittering phenomenon common to most SMC controllers. Also note that the actuator effort remains within the prescribed bounds of 75 N.

Additional simulations were run to test the controller's ability to handle parameter variations. Fig. 10 shows the system response to different k_1 values and Fig. 11 shows the response to different m_1 values. In all of these trials the controller parameters were kept the same even though the system parameters changed. Also note that both k_1 and m_1 were varied over the entire parameter range specified in Table II. The results clearly show that the control system is robust to parameter variation. This comes as no surprise because a SMC controller's greatest strength is its robustness to parameter variation.

B. Using the SMC Controller Without Command Generator

Since the SMC controller is robust to parametric uncertainties, it is natural to ask whether the ZVD command generator is necessary at all. Is the SMC controller robust enough to control both modes? The answer is no. Fig. V-B shows the response when the ZVD command generator is removed from the controller architecture. Mass m_1 has very good tracking, but mass m_2 shows large error and oscillation. Because mass m_2 is unobservable, the SMC controller is unable to sense and compensate for its oscillations. In addition, increasing the value of λ will not improve tracking in the unobservable mode. This clearly shows that

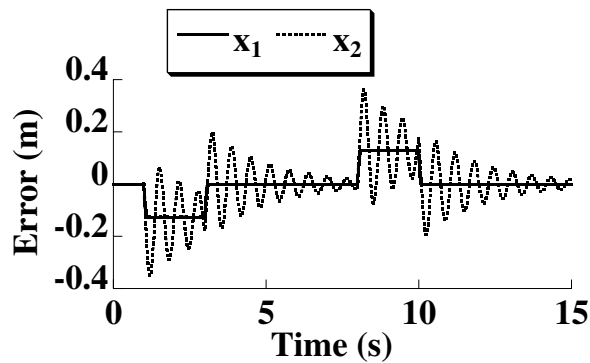


Fig. 12. SMC Controller Response (No ZVD Command Generation)

the command generator is an essential part of a successful control architecture.

VI. CONCLUSIONS

Many systems have unobservable modes whose response effects performance and task completion. For systems whose feedback control systems are developed without considering this unobservable mode, command shaping is an effective solution for reducing the vibration. This paper demonstrated that command shaping can be used with two different feedback control schemes: optimal PID control, and sliding mode control. For both of these control schemes, command shaping effectively eliminated the vibration from the unobservable mode.

REFERENCES

- [1] K. D. Young, V. I. Utkin, and U. Ozguner, "A control engineer's guide to sliding mode control," *IEEE Transactions on Control Systems Technology*, vol. 7, no. 3, pp. 328–342, 1999.
- [2] J.-J. E. Slotine and W. Li, *Applied Nonlinear Control*. Englewood Cliffs, New Jersey: Prentice Hall, 1991.
- [3] S.-H. Ryu and J.-H. Park, "Auto-tuning of sliding mode control parameters using fuzzy logic," in *American Control Conference*, Arlington, VA, 2001, pp. 618–623.
- [4] I. A. Shkolnikov and Y. B. Shtessel, "Causal nonminimum-phase tracking in nonlinear systems: Servocompensator enforced via sliding mode control," in *American Control Conference*, Arlington, VA, 2001, pp. 3642–3647.
- [5] E. A. Taha, G. S. Happaawana, and Y. Hurmuzlu, "Quantitative feedback theory (qft) for chattering reduction and improved tracking in sliding mode control," in *American Control Conference*, Arlington, VA, 2001, pp. 5004–5009.
- [6] J.-J. E. Slotine and S. S. Sastry, "Tracking control of non-linear systems using sliding surfaces, with application to robot manipulators," *Int. J. Control*, vol. 38, no. 2, pp. 465–492, 1983.
- [7] O. J. M. Smith, *Feedback Control Systems*. New York: McGraw-Hill Book Co., 1958.
- [8] P. H. Meckl and W. P. Seering, "Minimizing residual vibration for point-to-point motion," *Journal of Vibration, Acoustics, Stress and Reliability in Design*, vol. 107, pp. 378–382, 1985.
- [9] N. C. Singer and W. P. Seering, "Preshaping command inputs to reduce system vibration," *Journal of Dynamics, Systems Measurements and Control*, vol. 112, no. March, pp. 76–82, 1990.
- [10] V. Drapeau and D. Wang, "Verification of a closed-loop shaped-input controller for a five-bar-linkage manipulator," in *IEEE Int. Conf. on Robotics and Automation*, vol. 3. Atlanta, GA: IEEE, 1993, pp. 216–221.
- [11] D. P. Magee and W. J. Book, "Filtering micro-manipulator wrist commands to prevent flexible base motion," in *American Control Conf.*, Seattle, WA, 1995, pp. 924–928.
- [12] J. T. Feddema, "Digital filter control of remotely operated flexible robotic structures," in *American Control Conf.*, vol. 3. San Francisco, CA: ACC, 1993, pp. 2710–2715.
- [13] W. Singhose, L. Porter, M. Kenison, and E. Kriikku, "Effects of hoisting on the input shaping control of gantry cranes," *Control Engineering Practice*, vol. 8, pp. 1159–1165, 2000.
- [14] J. Fortgang, J. Marquez, and W. Singhose, "Application of command shaping on micro-mills," in *2004 Japan-USA Flexible Symposium on Automation*, Denver, CO, 2004.
- [15] S. Jones and A. G. Ulsoy, "An approach to control input shaping with application to coordinate measuring machines," *Journal of Dynamics, Measurement and Control*, vol. 121, pp. 242–247, 1999.
- [16] N. Seth, K. Rattan, and R. Brandstetter, "Vibration control of a coordinate measuring machine," in *IEEE Conf. on Control Apps.*, Dayton, OH, 1993, pp. 368–73.
- [17] W. E. Singhose, W. P. Seering, and N. C. Singer, "Improving repeatability of coordinate measuring machines with shaped command signals," *Precision Engineering*, vol. 18, pp. 138–146, 1996.
- [18] W. Singhose, N. Singhose, and W. Seering, "Time-optimal negative input shapers," *J. of Dynamic Systems, Measurement, and Control*, vol. 119, no. 3, pp. 198–205, 1997.
- [19] K. Hekman, J. Lawrence, and W. Singhose, "Using input shaping to suppress controller and structural oscillations," in *Mechatronics 2004 9th Mechatronics Forum*, Ankara, Turkey, 2004.